analytical chemistry

pubs.acs.org/ac Article

Study of Controlled Atmosphere Flexible Microtube Plasma Soft Ionization Mass Spectrometry for Detection of Volatile Organic Compounds as Potential Biomarkers in Saliva for Cancer

Pascal Vogel,[§] Constantinos Lazarou, Odhisea Gazeli, Sebastian Brandt, Joachim Franzke, and David Moreno-González*[,§]

Cite This: *Anal. Chem.* 2020, 92, 9722−9729 Read Online

ACCESS | Metrics & More | Article Recommendations | Supporting Information

ABSTRACT: A new soft ionization device for mass spectrometry is presented using the flexible microtube plasma under controlled atmospheric conditions. The controlled atmosphere flexible microtube plasma consists of the plasma source itself connected to a gas chromatograph and a mass spectrometer using a borosilicate glass cross piece. Controlled atmosphere, for example, nitrogen and/or an oxygen mixture, is introduced to the system to create a clean ionization environment. Reproducibility issues are discussed, and solutions are presented manipulating the gas flow in the cross piece. A proof of concept is shown using a ketone mixture introduced to the mass spectrometer to optimize atmospheric conditions. Furthermore, application of the presented device for the sensitive and nonfragmenting ionization of volatile organic biomarkers relevant for cancer is carried out. Sample treatment for human saliva is described, and relevant candidate biomarkers are measured in the saliva matrix, showing a very good ionization efficiency and neglectable matrix effects with limits of detection below 80 ppt.

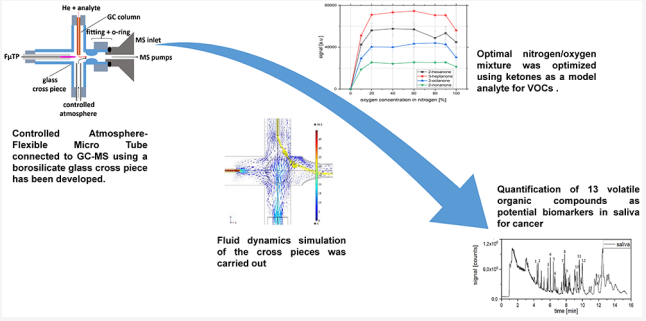

Within the past decade, atmospheric pressure plasmas are widely investigated within the research community because of their application as soft ionization sources for mass spectrometry (MS).[1−14] Many different approaches to increase the sensitivity and quality of these plasma-based ion sources have been proposed, such as manipulating the plasma gas,[15] the geometry,[16] or the distance from the mass spectrometer to the ionization source.[17] For the dielectric barrier discharge ionization (DBDI) source we recently demonstrated a significant increase in sensitivity and corresponding significantly improved limits of detection when using a controlled atmosphere (CA) setup.[18] This previous study was carried out using fluorinated compounds as model analytes in order to compare the CA-DBDI with the DBDI at open atmosphere. Within this study, two advantages were found: The controlled atmosphere significantly decreased the chemical noise in the mass spectrometer, and additionally, the atmosphere could be tailored for a certain class of analytes; thus, it could manipulate the chemical reaction pathways as it is beneficiary for the desired ionization process.

While plasma-based ionization sources have been improved within the past decade, also the challenges in their applications have become more complicated. This ionization source could be employed for the determination of candidate biomarkers in biological fluids. According to the National Cancer Institute (NCI), a biomarker is "a biological molecule found in blood, other body fluids, or tissues that is a sign of a normal or abnormal process, or of a condition or disease," such as cancer. Biomarkers typically differentiate an affected patient from a person without the disease.[19] In order to identify and measure biomarkers, e.g., for cancer, biological or biochemical samples have to be measured. These samples are usually very complicated biological matrixes, such as urine,[20,21] blood,[21] or saliva,[22] leading to a complex mass spectrum because of interfering species. In the case of volatile organic compounds (VOCs), the standard method to identify and quantify biomarkers using a gas chromatography-MS setup is electron ionization mass spectrometry (EI-MS). It covers a broad range of analytes with different polarities. Due to the high electron energy, on the order of 70 eV, widely used for this method, the observed ions are usually fragmented.

Thus, identification of the analytes is usually carried out by comparing the acquired mass spectra with spectral libraries, which are independent of the separation conditions. Normally,

Received: March 10, 2020
Accepted: June 24, 2020
Published: June 24, 2020

https://dx.doi.org/10.1021/acs.analchem.0c01063
Anal. Chem. 2020, 92, 9722−9729

every analyte is totally fragmented during ionization in GC-EI-MS. Thus, the molecular ion is often absent or can be detected with a very low intensity. Thus, quantification of the compounds with nonspecific fragmentation could be more complicated and less sensitive.[23,24] Therefore, it might be difficult to identify candidate biomarkers, especially at low concentrations. Although the coverage of EI databases is much more comprehensive compared to other databases which might be used for DBDI, such as ESI databases, the presence of molecular ions is clearly desirable. This is the case of coeluting compounds, where detection of one compound could be hidden below a more abundant interfering compound's fragmentation pattern. Analyzing different representative ketones with electron impact ionization, for example, can lead to the same fragmentation pattern for different analytes. Soft ionization mass spectrometry, as it is presented in this publication, may significantly simplify identification of each analyte, leading to better and more reliable detection methods.

In this study, we present a CA setup using the flexible microtube plasma ionization source (FμTP). With this setup, observed analytes are marginally fragmented and therefore more easily identified. Because of the controlled atmosphere, the influence of the surrounding atmosphere can be neglected, leading to less matrix effects in the measurement. Use of FμTP[16] allows one to reduce helium consumption by 1 order of magnitude and leads to an improvement in safe handling of the device because the high-voltage electrode is fully covered by the tubing.

Development of this new setup is presented, including design issues for a long-time reproducibility. This section is followed by an optimization part for the controlled atmosphere that is used. Finally, application of this setup to a complicated matrix, such as saliva, is shown, measuring 13 VOCs. It should be noted that the selected compounds were a subset of the 22 VOCs on a single-case/control study reported by Shigeyama et al.,[22] which were used as candidate biomarkers for oral cancer. The method presented in this work reaches limits of detection between 1.1 ppb and 80 ppt with a negligible matrix effect.

EXPERIMENTAL SECTION

Experimental Setup. *Flexible Microtube Plasma.* The plasma used in this study is the FμTP as it was first described by Brandt et al.[16] It is the next step in the development of dielectric barrier discharges applied for soft ionization mass spectrometry. It consists of a flexible polyimide-coated fused silica capillary with a 250 μm inner diameter and 360 μm outer diameter as shown Figure 1a. As a high-voltage electrode, a tungsten wire with an outer diameter of 100 μm is put into the fused silica capillary. The electrode wire ends 10 mm before the fused silica outlet. The plasma gas is flowing through the fused silica capillary and is therefore always in direct contact with the electrode. As presented by Brandt et al.,[16] it is behaving like a DBD with one electrode missing.

In this setup, a borosilicate glass cross piece is used to connect the MS inlet, the FμTP, the CA and the GC column in a center interaction point as shown in Figure 1a. The inner diameter of the cross piece is 2.4 mm with an outer diameter of 3.6 mm. The FμTP is driven with a rectangular voltage of 2.0 kV peak to peak with a frequency of 20 kHz. The cross piece is connected to the FμTP, CA, and GC column using Swagelok connectors (PFA-420-6-2). This gives the possibility to easily adapt the setup to any necessary change. In order to create a gastight atmosphere, the cross piece is installed on an in-house-

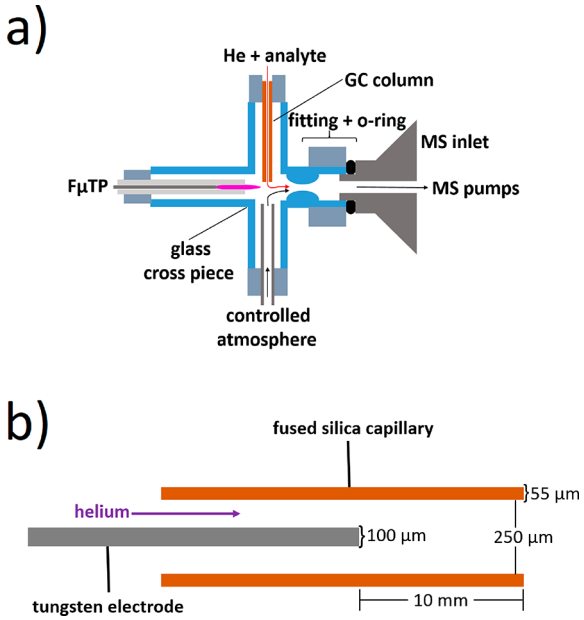

Figure 1. (a) Scheme of the glass cross piece connecting the FμTP, GC column, and mass spectrometer under controlled atmospheric conditions. Analytes introduced by the GC column are ionized by FμTP and measured by MS. (b) Dimensions of the FμTP design.

built stage that is mechanically connected to the mass spectrometer. Using an *XYZ*-stage, the cross peace is pressed against the mass spectrometer inlet. This connection is made gastight using an O-ring in the connection point. Helium flow through the FμTP is 100 sccm; CA can be varied between 0 and 2000 sccm. If not mentioned, CA flow was always 500 sccm with a mixture of 80% nitrogen and 20% oxygen. No part of the system besides the MS transfer tube and the GC oven was heated. Everything was kept at room temperature. Humidity was not artificially increased or reduced. GC conditions are explained in the gas chromatography section. In Figure 1a, a constriction between the gas flow crossing point and the mass spectrometer is shown. As this figure shows a cross section of the setup, the constriction in the cross point (z axis) cannot be seen. The mentioned constrictions are explained in the next section.

Reproducibility of the System. When we first carried out measurements under controlled atmospheric conditions using a symmetric glass cross piece without any constrictions as explained above, reproducibility issues were found after running the setup for a longer period of time. After several hours and several GC runs, the measured signals were no longer reproducible. In order to overcome this problem, it was crucial to understand the gas flow physics in the presented system. Fluid dynamic simulations as presented in Figure 2 could explain this irreproducibility issue: in Figure 2a and 2b, where no constrictions are in the cross section as well as in the connection to the mass spectrometer, it is clearly shown,that the GC flow is directed to the left wall of the cross and follows a circular motion before becoming entrained in the flow toward the mass spectrometer. Therefore, analytes may condense on the cold surfaces of the cross by extensive contact, resulting in irreproducibility and loss of sensitivity. In the Supporting Information, we also provide a velocity plot of the simulation and further information on how the simulations have been carried out. Figure 2c and 2d shows the difference in

https://dx.doi.org/10.1021/acs.analchem.0c01063
Anal. Chem. 2020, 92, 9722−9729

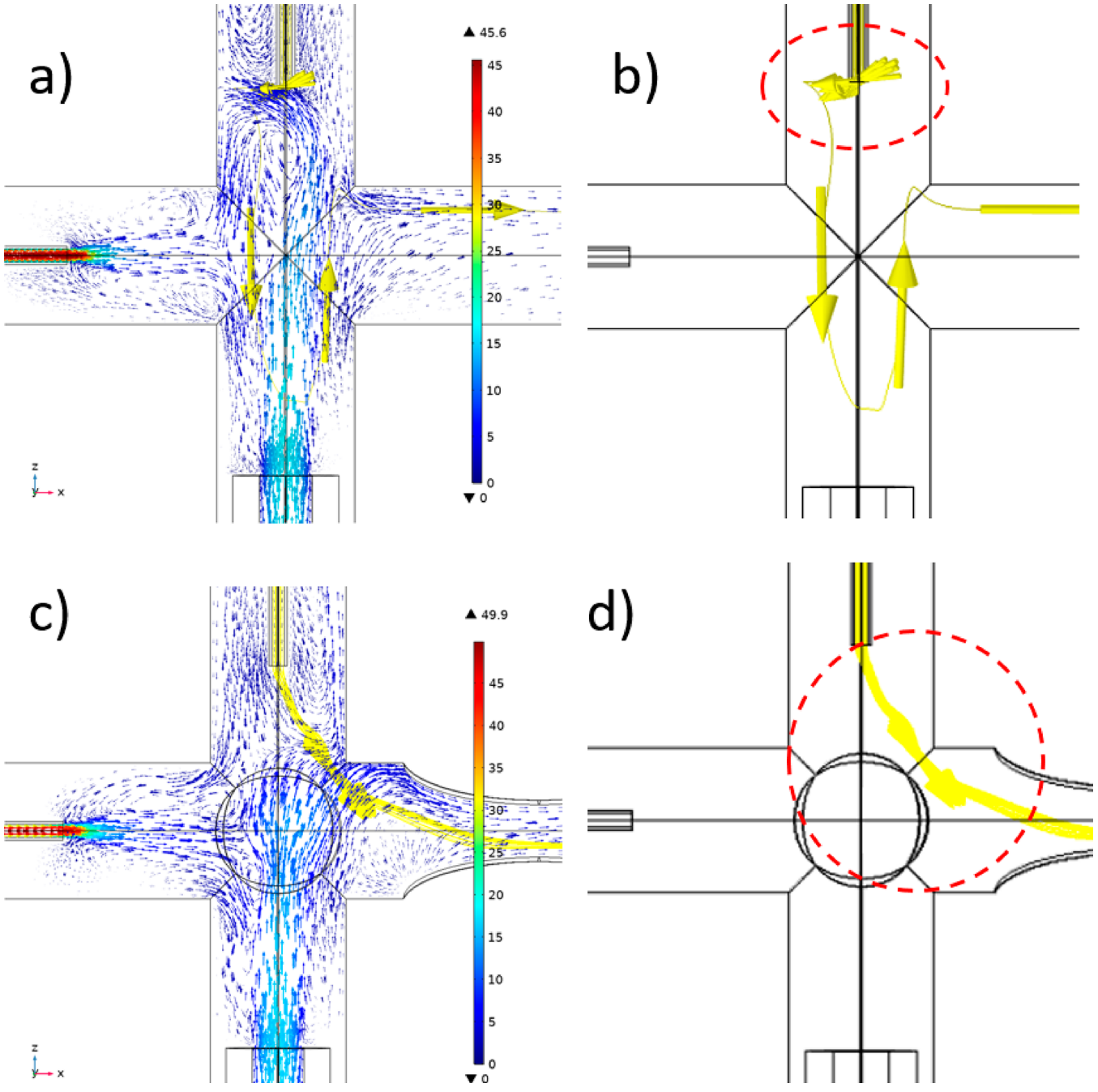

Figure 2. Fluid dynamics simulation of the cross pieces. (a) Velocity distribution of the gas flows (arrows) and distribution of the analyte from the GC column (yellow) for the cross piece without any constrictions. (b) Same as a without velocity arrows. (c) Velocity distribution of the gas flows (arrows) and distribution of the analyte (yellow) for the cross piece with constrictions. (d) Same as c without velocity arrows. Colored scale is in m/s.

these flows when the cross piece is constricted in the cross point (z axis in the picture) and in the connection to the mass spectrometer (y axis). To build this cross piece, a piece without constrictions was heated and then mechanically constricted when the glass was nearly liquid. The diameter of the middle of the cross piece was reduced to 0.3 mm in the z direction. In addition, the diameter of the connection to the mass spectrometer was symmetrically constricted to 1 mm. These changes have a large influence on the gas dynamics in the system, and the GC flow is directly reaching the mass spectrometer.

Operating the controlled atmosphere FμTP setup using the constricted cross piece led to a highly reliable reproducibility in all conducted measurements. This was proven by multiple measurements with the biomarker candidates described in Figure 5. Within multiple measurements over several months of a 100 ppb mixture of these analytes, the difference in signal intensities was always below 6%. The precision attained with the proposed approach was also evaluated over long runs involving +60 injections, achieving RSD values lower than 6% in all studied analytes. As could be observed in Figure S-1, the reproducibility for 3-octanone at 100 ppb was remarkable with a RSD of 5.4% (n = 6). Therefore, the presented setup in

https://dx.doi.org/10.1021/acs.analchem.0c01063
Anal. Chem. 2020, 92, 9722−9729

Figure 1 shows the constriction in the connection to the mass spectrometer. The constriction of the crossing point perpendicular to the glass tubes is not shown in Figure 1.

Gas Chromatography-Mass Spectrometry. An ion trap mass spectrometer with an atmospheric pressure inlet (Thermo Finnigan LTQ) was coupled to a gas chromatograph (Agilent Technologies 6890N) with a Restek gooseneck splitless liner (i.d. = 4 mm, o.d. = 6.5 mm, L = 78.5 mm) and 30 m Rxi-5 ms standard column (0.25 mm inner diameter, 0.25 μm film thickness). A 2 μL amount was injected by splitless mode with the injector temperature maintained at 200 °C and split opened after 1 min with a purge flow of 50 mL/min. The gradient profile was as follows: the oven temperature was held at 40 °C for 2 min and then heated to 160 °C in 10 min. The helium flow was 2 mL/min.

Chemicals. *n*-Hexane (purity > 98%) and 2-propanol (LC grade) were obtained from Merck KGaA (Darmstadt, Germany). Analytical standards of mesityl oxide, 1-hexanole, 4-methylphenole, 3-heptanone, 1-octen-3-ol, phenethyl alcohol. indole; dimethyl sulfone, 2-methoxythiophen, 2-hexanone, 3-octanone, 2-nonanone, and 1,2,4-trimethylbenzene were purchased from Sigma-Aldrich (ST. Louis, MO, USA). An individual standard solution of each compound was prepared in *n*-hexane or 2-propanol. Working standard solutions containing all compounds were prepared in *n*-hexane by proper dilution of the stock standard solutions.

Sample Collection and Treatment. Sample collection procedure was based on a previously reported work with some modifications.[22] Fresh human saliva samples were obtained from a nonsmoking male volunteer in our laboratory. The subject rinsed his mouth with water immediately prior to each sample collection. A 40 mL amount of unstimulated whole saliva was collected and mixed in a 50 mL glass bottle over a 24 h period. The sample was kept in the refrigerator at 4 °C until analysis. In order to prevent sample degradation, sample treatment was carried the after sample collection.

Sample treatment was as follows: 1 mL of saliva was placed in an Eppendorf tube. Then 100 μL of *n*-hexane was added to carry out the extraction, and this mixture was ultrasonicated for 10 min. To obtain a full separation of both phases, the mixture was centrifuged at 5000 rpm for 5 min. Finally, 2 μL of the organic layer was collected and directly injected into the GC-MS system. Using this procedure, a preconcentration factor of 10 was achieved.

RESULTS AND DISCUSSION

Optimization of Atmospheric Conditions. As many of the characteristic VOCs mentioned by Shigeyama et al.[22] are ketones or other hydrocarbons, we decided to use a ketone mixture as the model sample in order to test the system and to optimize atmospheric conditions. Different gas mixtures were tested, such as helium/nitrogen, helium/oxygen, and nitrogen/oxygen.

A nitrogen/oxygen mixture was found to be the best for ketones. In order to find the best mixing ratio between nitrogen and oxygen, a 100 ppb ketone mix was injected into the gas chromatograph and the signal intensities for the measured ion peaks in the chromatogram were evaluated. Different mixing ratios were tested, starting at 100% nitrogen and then successively increasing the oxygen amount up to 100% oxygen. The results are shown in Figure 3. Surprisingly, using pure nitrogen, no ions were measured in the experiment. Adding a small amount of oxygen directly led to a significant

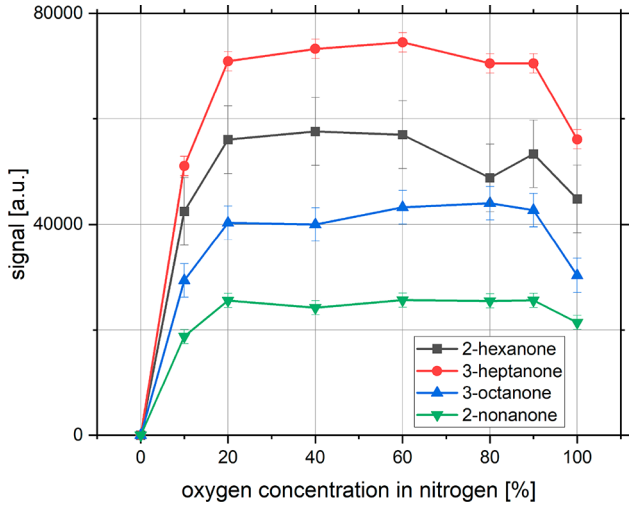

Figure 3. Variation of the oxygen concentration in a controlled atmosphere using ketones as model analytes to find optimal artificial atmospheric conditions for efficient soft ionization; 2 μL of a 100 ppb dilution of ketones in hexane was injected for every given oxygen concentration. Error bars calculated out of three replicate measurements.

ionization rate, resulting in a saturation effect at approximately 20% of oxygen in nitrogen. For a pure oxygen atmosphere, the ionization efficiency decreased slightly compared to lower oxygen amounts. As ketones are measured as $[M + H]^+$, the reaction pathway is probably dominated by the known protonation process: Following the ionization process for atmospheric pressure chemical ionization (APCI) sources, the main species involved in the production of positive ions using plasma-based ionization sources are nitrogen and water, forming protonated water clusters.[25]

$$N_2^+ + 2N_2 \rightarrow N_4^+ + N_2$$

$$N_4^+ + H_2O \rightarrow H_2O^+ + 2N_2$$

$$H_2O^+ + H_2O \rightarrow H_3O^+ + OH^\bullet$$

$$H_3O^+ + H_2O + N_2 \rightarrow H^+(H_2O)_2 + N_2$$

These water clusters then collide with an analyte, resulting in a proton transfer reaction as follows:

$$M + H^+(H_2O)_n \rightarrow MH^+ + (H_2O)_n$$

All of these equations do not require oxygen for the ionization process. In contrast to these equations, our measurements shown in Figure 3 demonstrate clearly that there is no ionization without adding oxygen to the controlled atmosphere. For a better understanding of Figure 3 and the processes responsible for the ionization, low-mass ions produced by the plasma without adding any analyte were measured while varying the oxygen concentration in the nitrogen-based controlled atmosphere. Measurement was carried out at different days and three times in total. The dependence of the signal on the oxygen concentration is shown in Figure 4 for NO^+ at m/z = 30 and $(H_2O)_2H^+$ at m/z = 37. Neither NO^+ nor $(H_2O)_2H^+$ was produced without adding oxygen to the controlled atmosphere, which is in very good agreement with the measurements presented in Figure 3.

Both measured ions show similar behavior depending on the oxygen concentration. Due to the fact that nitric oxide is most

https://dx.doi.org/10.1021/acs.analchem.0c01063
Anal. Chem. 2020, 92, 9722−9729

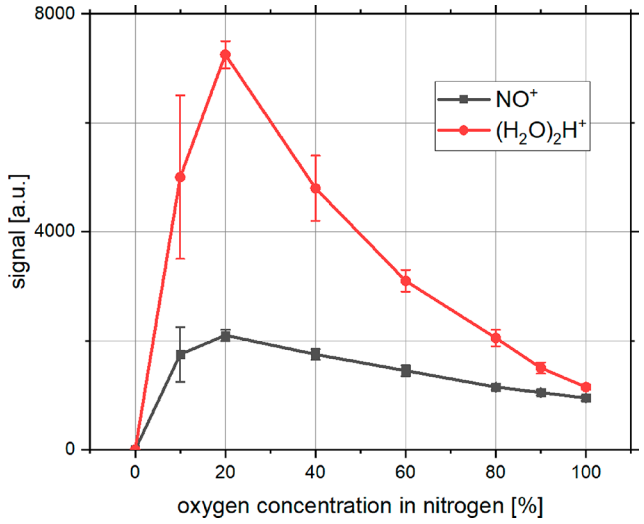

Figure 4. Measurement of ionized nitric oxide and protonated water clusters depending on the oxygen concentration in the nitrogen-based controlled atmosphere.

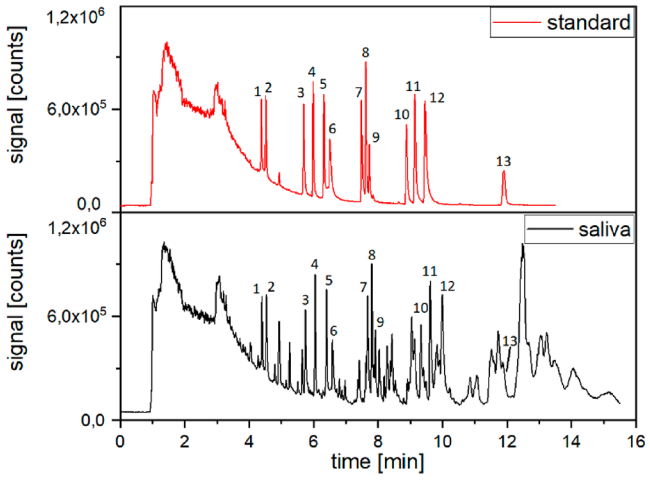

Figure 5. Comparison of total ion count chromatogram of 1 ppm of candidate biomarkers in hexane (standard) and 0.1 ppm of candidate biomarkers in a saliva matrix (1 ppm in the final extract because of the preconcentration factor of 10). Peaks 1−13 correspond to the following analytes: 1, 2-hexanone; 2, mesityl oxide; 3, 1-hexanole; 4, 3-heptanone; 5, 2-methoxythiophen; 6, dimethyl sulfone; 7, 1-octen-3-ol; 8, 3-octanone; 9, 1,2,4-trimethylbenzene; 10, 4-methylphenole, 11, 2-nonanone; 12, phenethyl alcohole; 13, indole.

probably formed by reactions with oxygen and nitrogen and the protonated water cluster ion peak shows exactly the same dependency, we suggest nitric oxide and in conclusion also oxygen to be an important species for the production of protonated water clusters in the presented setup. Comparing Figure 3 with Figure 4, the main difference in the curve progression is the saturation up to a concentration of 90% in Figure 3 and the signal decrease in Figure 4. A possible reason for this difference is very probably the low concentration of analyte injected in the measurements of Figure 3: Adding a small amount of oxygen to the controlled atmosphere creates already a sufficiently high amount of protonated water species to ionize most of the analyte, so that a further increase of protonated water species or a decrease does not affect the measurements anymore. Due to the maximum of both NO^+ and protonated water cluster production for 20% of oxygen concentration in nitrogen, we decided to choose this as the optimum condition for further experiments.

Analytical Performance. In order to show the capability and performance of the presented setup for determination of candidate biomarkers for oral cancer, standard and matrix-matched calibration curves were prepared. Concentrations from 1 to 1000 and from 0.1 to 100 ppb were measured in the case of standard calibration and matrix-matched calibration, respectively. A chromatogram representing the total ion count of the mass spectrometer can be seen in Figure 5, showing both biomarkers in standard dilution and in a saliva matrix.

The matrix effect is a key aspect for obtaining reliable results in GC-MS analysis.The analytical response could be enhanced or decreased by coextractants present in the final extract. Thus, the matrix effect was evaluated by comparing the slopes of the matrix-matched calibration curves prepared from blank sample extracts to those of external calibration curves of standard solutions at the same concentration levels using the following equation:[26] matrix effect (%) = [(slope of matrix-matched calibration/slope of external standard calibration) − 1] × 100. A matrix effect of zero means that the signal or suppression or enhancement has not been observed. A table of the matrix effects for all compounds is shown in the Supporting Information (Table S-1). All measured compounds showed negligible matrix effects with values from −5% to −1% in all cases. For instance, indole coeluted with a considerable number of interfering species from the matrix (Figure 5). However, this analyte presented a matrix of −4, which means that it does not effect the ionization process. Thus, the high reproducibility of the system even for different sample matrixes has been shown. Although many additional peaks occur for measurements in the saliva matrix, this hardly has an influence on the detection, identification, and quantification of the observed candidate biomarkers because of the soft ionization technique resulting from the FμTP. This benefit results in a more reliable identification of the studied analytes due to their presence being hidden below a more abundant interfering compound's fragmentation pattern. LODs are shown in Table 1 with instrumental LODs from 10 ppb for 2-hexanone to 700 ppt for 3-octanone and 2-nonanone. LODs from matrix-matched calibration in saliva were lower than 1100 ppt in all cases, taking into account the preconcentration factor of 10.

Although 2-hexanone, 3-heptanone, 3-octanone, and 2-nonanone are all ketones, the instrumental LODs for 2-hexanone and 3-heptanone are significantly higher compared to 3-octanone and 2-nonanone. This is due to the fact that the solvent hexane causes a broad background in the signal from approximately 1 to 5 min. Most relevant retention times for this background are between 1 and 3 min, but between 3 and 5 min the noise of this background still affects LODs for compounds that have an $[M + H]^+$ in the range of 80−120 amu, as is the case for 2-hexanone and 3-heptanone. As 3-octanone and 2-nonanone have retention times higher than 5 min and are measured at 129 and 143 m/z, respectively, they are not influenced by this effect and show excellent limits of detection in the ppt range.

Soft Ionization Compared to Electron Impact Ionization. As already mentioned in the introduction of this publication, the main advantage of soft ionization methods compared to the standard procedure for GC-MS measurements that is currently EI ionization avoids fragmentation of analyte ions. To demonstrate this advantage of the presented system, EI mass spectra from mesityl oxide found in the

https://dx.doi.org/10.1021/acs.analchem.0c01063
Anal. Chem. 2020, 92, 9722−9729

Table 1. Limits of Detection for Candidate Biomarkers Obtained from External Standard Calibration and Matrix-Matched Calibration

analyte	observed peak [m/z]	LOD from external standard calibration [ppb]	LOD from matrix matched calibration in saliva[a] [ppb]
2-hexanone	101	10	1.1
mesityl oxide	99	5	0.4
1-hexanole	103	6	0.5
3-heptanone	115	8	0.9
2-methoxythiophen	115	2	0.2
dimethyl sulfone	95	9	0.9
1-octen-3-ol	129	1	0.09
3-octanone	129	0.7	0.08
1,2,4-trimethylbenzene	121	3	0.3
4-methylphenol	109	0.8	0.08
2-nonanone	143	0.7	0.08
phenethyl alcohol	123	9	0.9
indole	118	2	0.18

[a]Matrix-matched calibration curves were obtained by spiking blank samples at different concentrations before sample treatment. Thus, the obtained LODs take into account a preconcentration of 10.

literature[27] are compared to the mass spectra obtained using the presented CA-FμTP ion source. The CA-FμTP spectrum for mesityl oxide is shown in Figure 6.

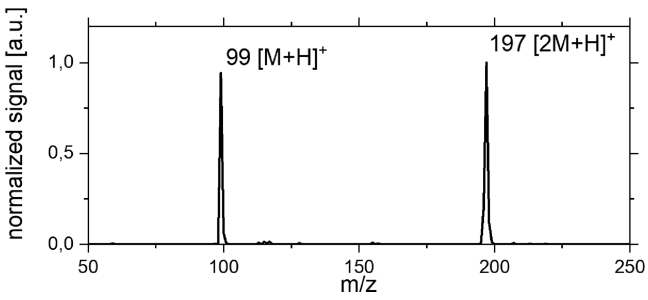

Figure 6. Soft ionization spectra of the CA-FμTP for 1 ppm mesityl oxide showing the $[M + H]^+$ and the $[2M + H]^+$ peaks.

Comparing Figure 6 to the spectra obtained in the literature[27] or that can be found in common EI MS databases such as NIST, the potential of plasma-based soft ionization becomes clear. Because there is no fragmentation, analyte identification and also quantification and sensitivity are significantly improved compared to electron impact ionization methods. In the case of mesityl oxide, the presented method is approximately 2.5 times more sensitive than the cited method taking into account that the referenced method uses a 1 μL injection and a 1:1 split ratio while the manuscript uses 2 μL injection and splitless injection. To show these aspects, the mass spectrum obtained by EI-MS can also be found in the Supporting Information (Figure S-2) together with a total ion count chromatogram of a standard solution at 1 ppm that was injected to a Agilent 7890A GC system coupled to an Agilent 5975C inert XL MSD mass spectrometer using the same GC conditions (Figure S-3)

Comment on Application of Obtained Results. In the optimization section of the presented work, an optimum for the soft ionization efficiency of the setup was found at a mixture of 80% nitrogen and 20% oxygen. As this is approximately the mixture of the ambient air, further experiments were carried out to understand the significant improvements of controlled atmosphere setups compared to ionization sources at ambient air. Ambient air consists of approximately 78% nitrogen, 21% oxygen, 0.9% argon, and 0.1% other gases. A synthetic air (commercial 80% nitrogen, 20% oxygen) mixture was tested as well. In a next step, 1% argon was added to this commercially available synthetic air and the experiment was repeated. With this experiment, the three main compounds of air have been introduced to the system. As a last step, ambient air from the laboratory was used instead of synthetic air. Flows were always kept constant at a flow rate of 500 sccm. Results are shown in Figure 7 for 100

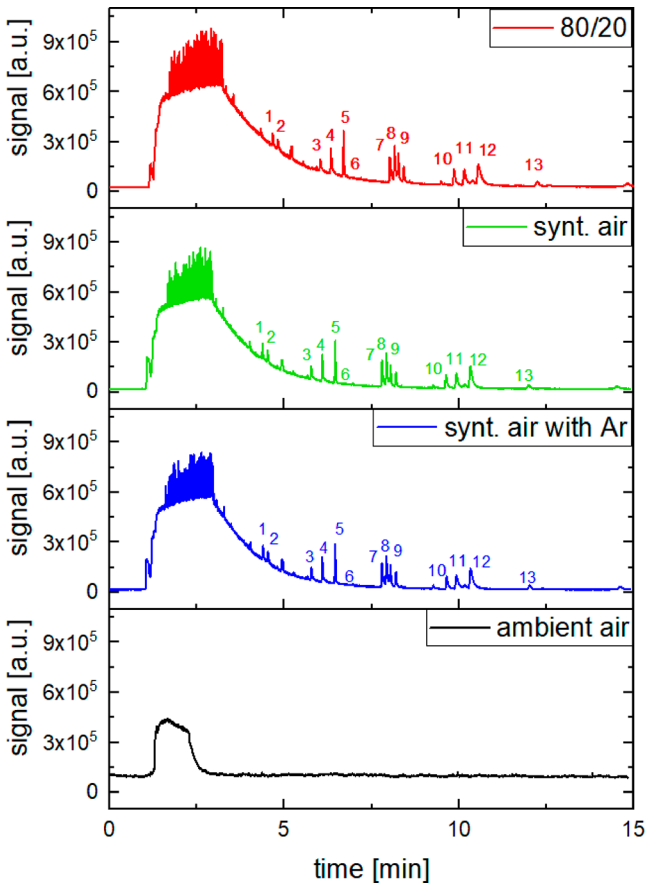

Figure 7. Comparison of total ion count for different controlled atmospheric conditions measuring 100 ppb of candidate biomarker standard dilution. Online mixing (80/20) and use of synthetic air and synthetic air with 1% argon show similar results. Using a controlled amount of ambient air from the laboratory, a significant decrease in signal appears. Analytes could no longer be quantified or detected under these conditions. Numbers in belong to the analytes as follows: 1, 2-hexanone; 2, mesityl oxide; 3, 1-hexanole; 4, 3-heptanone; 5, 2-methoxythiophen; 6, dimethyl sulfone; 7, 1-octen-3-ol; 8, 3-octanone; 9, 1,2,4-trimethylbenzene; 10, 4-methylphenole, 11, 2-nonanone; 12, phenethyl alcohole; 13, indole.

ppb candidate biomarker standard dilution. The 80% nitrogen with 20% oxygen mixture obtained by two mass flow controllers, synthetic air (only one MFC necessary) and synthetic air with argon, shows similar results. All analytes could be detected. It is important to mention that analyte 6 is not seen in the total ion count chromatogram but can easily be detected by observing m/z = 95. Using ambient air from the

https://dx.doi.org/10.1021/acs.analchem.0c01063
Anal. Chem. 2020, 92, 9722−9729

laboratory, candidate biomarkers could no longer be measured at this concentration. Comparing the baseline of ambient air with the baseline in the other chromatograms, the baseline for the ambient air measurement is 5 times higher. As a conclusion, ambient air is polluted by many different species resulting in a high chemical background that reduces the sensitivity of the system for the analytes that have to be measured. In the Supporting Information we show the mass spectrum of the baseline for both ambient air and synthetic air. As could be observed in Figure S-4, the most abundant was m/z 74 in the case of ambient air whereas this ion was not detected in synthetic air. Its origin could correspond to acetonitrile and methanol $[(CH_3CN)(CH_3OH) + H]^+$. These solvents are commonly used in an analytical chemistry laboratory. Thus, their presence in the ambient mass spectrum is justified. This shows the advantage of controlling the atmosphere: A clean ionization environment reduces the chemical noise, leading to a significantly more efficient and therefore more sensitive detection of the analytes.

CONCLUSIONS

The CA-FμTP was presented as a further development of the CA-DBDI ion source for mass spectrometry. Understanding and controlling the gas flows were found to be crucial parameters for reproducible long-time measurements. Following previous publications, oxygen was found to be an important part of the ionization atmosphere for high-sensitivity measurements. The optimal nitrogen/oxygen mixture was measured using ketones as a model analyte for VOCs as candidate biomarkers relevant for oral squamous cell cancer. Using these optimized conditions for detection of candidate biomarkers resulted in instrumental LODs in the range of 0.7−10 ppb for all analytes, hereas LODs in saliva ranged from 0.08 to 1.1 ppb, taking into account a preconcentration factor of 10. Comparing the LODs of the presented work with LODs of other methods in the literature, depending on the analyte, an improvement of 2.5 times was found. It was demonstrated that use of ambient air for detection of the analytes led to a significant decrease of the signal, resulting in a worse sensitivity of the system. Therefore, the CA-FμTP ionization source is a very promising tool for both sensitive analysis of VOCs and to study the mechanisms of plasma-based ionization techniques.

ASSOCIATED CONTENT

Supporting Information

The Supporting Information is available free of charge at https://pubs.acs.org/doi/10.1021/acs.analchem.0c01063.

Peak area precision for 3-octanone at 100 ppb in solvent; EI-MS mass spectrum of mesityl oxide; total ion count chromatogram of EI-MS measurement of the characteristic volatiles; mass spectra for the baselines of Figure 7; boundary conditions for the fluid dynamics simulations of Figure 2; schematic diagram of the device, and pressure across the device; boundary velocity magnitude for the glass cross piece without constrictions; boundary velocity magnitude for the glass cross piece with constrictions; slope of the external standard calibration and matrix-matched calibration, and matrix effect of each studied analyte (PDF)

AUTHOR INFORMATION

Corresponding Author

David Moreno-González − *ISAS-Leibniz-Institut für Analytische Wissenschaften, Dortmund 44139, Germany;* orcid.org/0000-0002-3292-7308; Email: david.moreno@isas.de

Authors

Pascal Vogel − *ISAS-Leibniz-Institut für Analytische Wissenschaften, Dortmund 44139, Germany;* orcid.org/0000-0002-9867-1413

Constantinos Lazarou − *FOSS Research Centre for Sustainable Energy, PV Technology, University of Cyprus, Nicosia 1678, Cyprus*

Odhisea Gazeli − *FOSS Research Centre for Sustainable Energy, PV Technology, University of Cyprus, Nicosia 1678, Cyprus*

Sebastian Brandt − *ISAS-Leibniz-Institut für Analytische Wissenschaften, Dortmund 44139, Germany;* orcid.org/0000-0002-6938-3033

Joachim Franzke − *ISAS-Leibniz-Institut für Analytische Wissenschaften, Dortmund 44139, Germany;* orcid.org/0000-0003-0419-1898

Complete contact information is available at: https://pubs.acs.org/10.1021/acs.analchem.0c01063

Author Contributions

§P.V. and D.M.-G.: These authors contributed equally to this work.

Notes

The authors declare no competing financial interest.

ACKNOWLEDGMENTS

Financial support from the Ministerium für Kultur und Wissenschaft des Landes Nordrhein-Westfalen, the Senatskanzlei des Landes Berlin, and the Bundesministerium für Bildung und Forschung is gratefully acknowledged. This project received funding from the European Union's Horizon 2020 research and innovation program under grant agreement 810686 and under the Marie Sklodowska-Curie grant agreement number 840743. We gratefully acknowledge the highly competent support from the scientific glass workshop of the Technische Universität Dortmund in combination with the construction and design of the glass cross piece.

REFERENCES

(1) Andrade, F. J.; Shelley, J. T.; Wetzel, W. C.; Webb, M. R.; Gamez, G.; Ray, S. J.; Hieftje, G. M. *Anal. Chem.* **2008**, *80* (8), 2654−63.

(2) Andrade, F. J.; Shelley, J. T.; Wetzel, W. C.; Webb, M. R.; Gamez, G.; Ray, S. J.; Hieftje, G. M. *Anal. Chem.* **2008**, *80* (8), 2646−53.

(3) Badal, S. P.; Michalak, S. D.; Chan, G. C. Y.; You, Y.; Shelley, J. T. *Anal. Chem.* **2016**, *88* (7), 3494−3503.

(4) Badal, S. P.; Ratcliff, T. D.; You, Y.; Breneman, C. M.; Shelley, J. T. *J. Am. Soc. Mass Spectrom.* **2017**, *28* (6), 1013−1020.

(5) Bregy, L.; Sinues, P. M.; Nudnova, M. M.; Zenobi, R. *J. Breath Res.* **2014**, *8* (2), 027102.

(6) Cody, R. B.; Laramee, J. A.; Durst, H. D. *Anal. Chem.* **2005**, *77* (8), 2297−2302.

(7) Gyr, L.; Wolf, J. C.; Franzke, J.; Zenobi, R. *Anal. Chem.* **2018**, *90* (4), 2725−2731.

(8) Hagenhoff, S.; Franzke, J.; Hayen, H. *Anal. Chem.* **2017**, *89* (7), 4210−4215.

(9) Hagenhoff, S.; Korf, A.; Markgraf, U.; Brandt, S.; Schutz, A.; Franzke, J.; Hayen, H. *Rapid Commun. Mass Spectrom.* **2018**, *32* (13), 1092−1098.
(10) Klute, F. D.; Michels, A.; Schutz, A.; Vadla, C.; Horvatic, V.; Franzke, J. *Anal. Chem.* **2016**, *88* (9), 4701−5.
(11) Klute, F. D.; Schutz, A.; Brandt, S.; Burhenn, S.; Vogel, P.; Franzke, J. *J. Phys. D Appl. Phys.* **2018**, *51* (31), 314003.
(12) Lara-Ortega, F. J.; Robles-Molina, J.; Brandt, S.; Schutz, A.; Gilbert-Lopez, B.; Molina-Diaz, A.; Garcia-Reyes, J. F.; Franzke, J. *Anal. Chim. Acta* **2018**, *1020*, 76−85.
(13) Mirabelli, M. F.; Wolf, J. C.; Zenobi, R. *Analyst* **2017**, *142* (11), 1909−1915.
(14) Shelley, J. T.; Chan, G. C. Y.; Hieftje, G. M. *J. Am. Soc. Mass Spectrom.* **2012**, *23* (2), 407−417.
(15) Schütz, A.; Lara-Ortega, F. J.; Klute, F. D.; Brandt, S.; Schilling, M.; Michels, A.; Veza, D.; Horvatic, V.; García-Reyes, J. F.; Franzke, J. *Anal. Chem.* **2018**, *90* (5), 3537−3542.
(16) Brandt, S.; Klute, F. D.; Schutz, A.; Marggraf, U.; Drees, C.; Vogel, P.; Vautz, W.; Franzke, J. *Anal. Chem.* **2018**, *90* (17), 10111−10116.
(17) Pu, J.; Dai, J.; He, F.; Zhu, S.; Zhao, Z.; Duan, Y. *J. Am. Soc. Mass Spectrom.* **2020**, *31* (3), 752−762.
(18) Vogel, P.; Marggraf, U.; Brandt, S.; Garcia-Reyes, J. F.; Franzke, J. *Anal. Chem.* **2019**, *91* (5), 3733−3739.
(19) Henry, N. L.; Hayes, D. F. *Mol. Oncol.* **2012**, *6*, 140−146.
(20) Silva, C. L.; Passos, M.; Camara, J. S. *Talanta* **2012**, *89*, 360−8.
(21) Filipiak, W.; Mochalski, P.; Filipiak, A.; Ager, C.; Cumeras, R.; Davis, C. E.; Agapiou, A.; Unterkofler, K.; Troppmair, J. *Curr. Med. Chem.* **2016**, *23* (20), 2112−2131.
(22) Shigeyama, H.; Wang, T.; Ichinose, M.; Ansai, T.; Lee, S. W. *J. Chromatogr. B: Anal. Technol. Biomed. Life Sci.* **2019**, *1104*, 49−58.
(23) Portolés, T.; Mol, J. G. J.; Sancho, J. V.; Hernández, F. *Anal. Chem.* **2012**, *84*, 9802−9810.
(24) Mirabelli, M. F.; Wolf, J. C.; Zenobi, R. *Analyst* **2017**, *142*, 1909−1915.
(25) Andrade, F. J.; Shelley, J. T.; Wetzel, W. C.; Webb, M. R.; Gamez, G.; Ray, S. J.; Hieftje, G. M. *Anal. Chem.* **2008**, *80* (8), 2646−2653.
(26) Matuszewski, B. K.; Constanzer, M. L.; Chavez-Eng, C. M. *Anal. Chem.* **2003**, *75* (13), 3019−30.
(27) Peng, M.; Wen, H.; Le, J.; Yang, Y. *Anal. Methods* **2012**, *4* (12), 4063−4067.

https://dx.doi.org/10.1021/acs.analchem.0c01063
Anal. Chem. 2020, 92, 9722−9729